Adding Alumina Nanoparticles to Enhance Falling Film Evaporation

Xiaoming Cui*

Department of Mechanical and Electrical Engineering, Jinan Engineering Polytechnic, Jinan, 250200 China

*Corresponding author's e-mail: beee@188.com

Abstract. Falling film evaporation is widely applied in chemical processes, refrigeration, and seawater desalination, with its heat transfer efficiency playing a crucial role in the energy utilization of these systems. However, unstable liquid film formation and heat transfer bottlenecks during evaporation often limit its performance. In recent years, nanofluids, due to their high thermal conductivity and heat capacity, have emerged as a potential solution to enhance heat transfer efficiency. This study develops a two-dimensional mathematical model based on the Volume of Fluid (VOF) method to analyze the effects of adding 3% aluminum oxide (Al_2O_3) nanoparticles on liquid film thickness, heat transfer coefficient, and evaporation rate under different Reynolds numbers (Re = 600 ~ 2400). The results show that, compared to water, nanofluids significantly increase film thickness and improve heat transfer and evaporation efficiency under higher Re conditions. At Re = 1200, the liquid film temperature reaches its peak, but further increases in Re reduce the evaporation rate due to the growth of film thickness. This study offers new insights and theoretical guidance for optimizing falling film evaporation systems using nanofluids.

Keywords: Falling film; Nanoparticles; Thickness; Mass transfer rate

1 Introduction

Falling film evaporation is an efficient heat transfer technology widely used in chemical engineering, refrigeration, and seawater desalination, with its heat transfer efficiency directly impacting the energy utilization of these systems [1]. However, traditional falling film evaporation often faces limitations in heat transfer efficiency during practical applications, particularly due to unstable liquid film formation and heat transfer bottlenecks during evaporation. In recent years, the introduction of nanofluids has revealed that adding nanoparticles to the working fluid can significantly enhance heat transfer performance [2-3]. Nanofluids, due to their unique thermal properties, including higher thermal conductivity and greater heat capacity, have become a potential solution for improving heat transfer efficiency.

Numerous studies have been conducted on various types of nanofluids. For instance, researchers have observed significant increases in heat transfer coefficients by adding

W. He et al. (eds.), *Proceedings of the 2024 10th International Conference on Advances in Energy Resources and Environment Engineering (ICAESEE 2024)*, Atlantis Highlights in Engineering 36,
https://doi.org/10.2991/978-94-6463-708-3_30

nanoparticles such as copper oxide (CuO), titanium dioxide (TiO_2), and silica (SiO_2) to base fluids like water and ethylene glycol. Hoffmann et al. [4] conducted experiments on falling film absorption in horizontal tubes, discovering that the falling film heat transfer coefficient peaked at an additive concentration of 40 ppm. Under varying additive concentrations and mass flow rates of LiBr aqueous solution, the heat transfer coefficient increased by 60% to 140%. Qi [5] found that the addition of isooctanol and nanoparticles enhanced the ability of lithium bromide solution to absorb water vapor; at an absorption pressure of 1.6 kPa, the mass transfer coefficient when adding 1% isooctanol was 1.74 times that of pure lithium bromide solution and 1.32 times that of nanofluid lithium bromide solution. Jiang et al. [6] investigated the effect of different amounts of titanium dioxide nanoparticles on the coefficient of performance (COP) of an ammonia-water absorption refrigeration system (AARS), concluding that titanium dioxide nanoparticles significantly impact the AARS, with a COP increase of 27 %. Among various nanofluids, a mixture of 0.5% titanium dioxide and 0.02% SDBS exhibited the most significant improvement in COP.

Despite the extensive research on the enhanced heat and mass transfer effects of nanofluids in falling film evaporation, previous studies predominantly focused on absorption refrigeration systems using lithium bromide or ammonia-water solutions, with a notable gap in research regarding the enhancement of falling film evaporation using nanoparticles in water. Therefore, this study establishes a two-dimensional mathematical model for falling film evaporation, analyzing the effects of adding aluminum oxide (Al_2O_3) nanoparticles on liquid film thickness, heat transfer coefficients, and evaporation rates. This research provides new insights and theoretical foundations for further improving the performance of falling film evaporation systems.

2 Material and Method

2.1 Physical and Boundary Condition

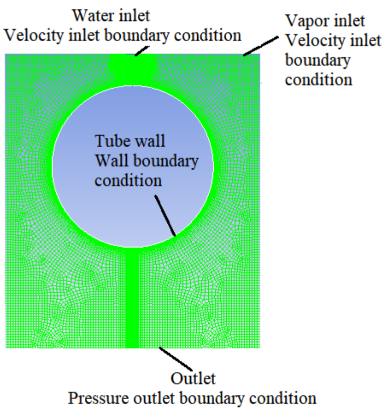

Fig. 1. Meshing physical model with boundary conditions

The two-dimensional physical model of the falling film evaporator is shown in Figure 1. In this figure, the diameter of the horizontal tube is 25.4 mm. The surface of the horizontal tube is set with a wall boundary condition at a temperature of 62 °C. There is a liquid distribution inlet on the upper side of the horizontal tube, measuring 2 mm in length. This inlet is defined as a velocity inlet boundary condition, with water flow rates set in the range of 0.037 kg/s to 0.148 kg/s (Re = 600 to 2400). Liquid water, under the influence of gravity, falls onto the top of the horizontal tube. Subsequently, a liquid film forms on the outer surface of the horizontal tube due to the combined effects of gravity, viscous forces, and surface tension, continuously absorbing the heat released from the tube and generating water vapor. The physical property parameters of the materials in the model are listed in Table 1.

Table 1. Physical properties of fluids [7-8]

Name	Density kg/m^3	Specific heat capacity J/(kg·K)	Thermal conductivity W(/m· K)	Dynamic viscosity Pa· s
Nanofluid	1073	3797.8	0.73	0.000645
Vapor	0.1304	1966.4	0.02119	1.1×10^{-5}
Water	983.1	4182.9	0.60	0.000466

2.2 Governing Equation

In the numerical simulation of falling film evaporation, the Volume of Fluid (VOF) method is used to track the dynamic changes of the gas-liquid interface, combined with the Lee evaporation model to describe the liquid phase evaporation process. Before conducting the numerical simulation, reasonable assumptions must be made for the model, including the following points: (1) The surface tension and curvature of the gas-liquid interface remain constant, with the Continuum Surface Force (CSF) model applied to handle the surface tension effects at the interface; (2) The physical properties of the liquid and gas (such as density, viscosity, thermal conductivity, etc.) are kept constant throughout the flow process; (3) The shear stress of water vapor on the liquid film flow is neglected.

The following are the governing equations established for the mathematical model:

$$\frac{\partial \alpha}{\partial t}+\nabla\cdot\left(\alpha\vec{v}\right)=\frac{\dot{m}_{evap}}{\rho_l} \tag{1}$$

$$\frac{\partial}{\partial t}\left(\rho\vec{v}\right)+\nabla\cdot\left(\rho\vec{v}\vec{v}\right)=-\nabla p+\nabla\left[\mu\nabla\vec{v}\right]+\rho\vec{g}+\vec{F}_{st} \tag{2}$$

$$\frac{\partial}{\partial t}\left(\rho h\right)+\nabla\cdot\left(\rho h\vec{v}\right)=\nabla\cdot\left(k_{eff}\nabla T\right)+\dot{q}_{evap} \tag{3}$$

The evaporation rate of the liquid film in Equation (1) can be obtained using the Lee evaporation model (Equation (4)).

$$\dot{m}_{evap} = C_{evap} \frac{\rho_l (T - T_{sat})}{T_{sat}} \alpha \tag{4}$$

3 Results and Conclusion

3.1 Simulation Verification

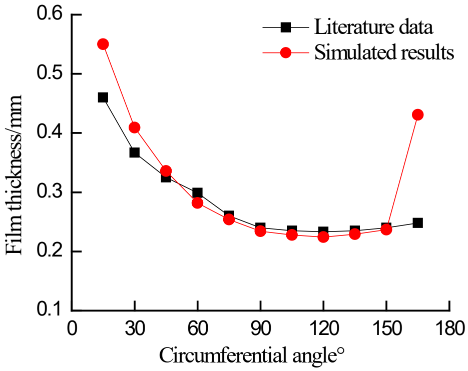

Fig. 2. Comparison between literature and simulation values of liquid film thickness

Figure 2 compares the literature values [9] with the simulated values of the liquid film thickness outside the horizontal tube when Re = 1250. From Figure 2, it can be observed that the simulated values align well with the literature values in the range of circumferential angles from 30° to 150°. The relative deviation between the simulated and literature values primarily occurs for circumferential angles less than 30° and greater than 150°. The deviation observed in the region where the circumferential angle is less than 30° arises because the liquid height in the literature [9] is lower than that in this study, resulting in a higher kinetic energy of the liquid when it contacts the horizontal tube in this research.

3.2 Film Thickness

In the study of falling film evaporation, analyzing the local liquid film thickness is essential. The thickness of the liquid film directly influences the efficiency of heat and mass transfer, thereby affecting the evaporation rate and the overall performance of the system. By accurately measuring and analyzing the local liquid film thickness, we can identify optimal operating conditions, optimize equipment design, and enhance energy utilization efficiency. Furthermore, understanding the variations in liquid film thickness can help predict drying and scaling phenomena, thus improving the system's reliability and stability.

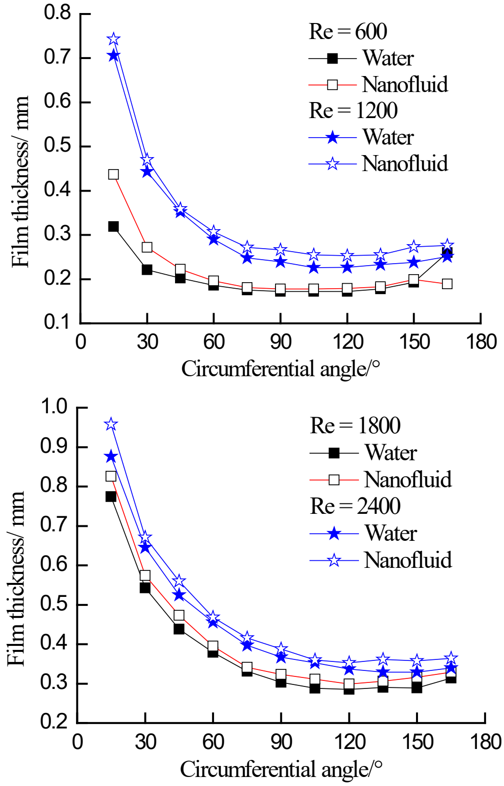

Fig. 3. Film thickness with respect to circumferential angle

Figure 3 illustrates the variation of local liquid film thickness along the circumferential direction of a horizontal tube, using nanofluid and water as working fluids within the range of Re=600 ~ 24002. From the figure, it is evident that the film thickness of the nanofluid is greater than that of water across this range. This can be attributed to the higher viscosity of the nanofluid compared to water, which hinders the spreading of the liquid film and results in increased thickness. Specifically, at Re values of 600, 1200, 1800, and 2400, the film thickness of the nanofluid increased by 27.31% to 36.99%, 1.99 % to 14.71 %, 3.02 % to 9.34 %, and 1.98 % to 9.73% compared to water, respectively. It is noteworthy that, except for the case of Re=600Re = 600Re=600, the effect of nanomaterial particles on film thickness remains relatively unchanged with increasing Re. This may be due to the more laminar flow state at lower Re values (such as 600), where the influence of the nanoparticles on the liquid film is more pronounced, leading to a significant reduction in film thickness. In contrast, at higher Re values, the flow gradually transitions to turbulence, enhancing the fluid's kinetic energy and diminishing the effect of nanoparticles, resulting in a smaller variation in film thickness. This indicates that the influence of nanoparticles on film thickness does not significantly change with increasing Re.

3.3 Liquid Temperature

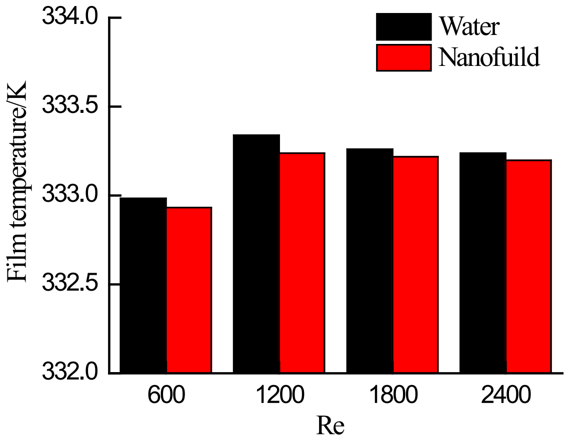

Fig. 4. Liquid temperature for different Re

Figure 4 presents the average temperatures of the nanofluid and water outside the horizontal tube. It can be observed that as the Re increases, the average temperature of both the nanofluid and water first rises, reaching a peak at Re = 1200, and then gradually decreases when Re exceeds 1200. As Re increases, the velocity within the liquid film also increases, leading to an enhanced heat transfer rate between the tube wall and the liquid film, which in turn raises the temperature of the liquid film. However, with further increases in Re, the liquid film thickness continues to grow, resulting in a greater amount of heat required to raise the temperature of the outer liquid film, causing a gradual decrease in its temperature. A comparative analysis of the average temperatures of the nanofluid and water reveals that, within the range of Re= 600 to 2400, the temperature of water is consistently slightly higher than that of the nanofluid. This can be attributed to the fact that although the thermal conductivity of the nanofluid is greater than that of water, which enhances heat transfer between the liquid film and the tube wall, thereby increasing the temperature of the liquid film, the thicker liquid film of the nanofluid and its higher viscosity, as shown in Figure 3, result in lower velocities compared to the water film. This ultimately leads to a cooling effect in the nanofluid film.

3.4 Mass Transfer Rate

While extensive research has analyzed the heat transfer enhancement effects of nanofluids, most studies have focused on unidirectional heat transfer and have not directly demonstrated the effects of nanofluids on evaporation enhancement. To better illustrate the effectiveness of nanofluids in enhancing falling film evaporation, Figure 5 presents the evaporation rates (mass transfer rates) during falling film evaporation using nanofluids and water as working fluids within the Reynolds number range of 600 to 2400. From Figure 5, it can be observed that as the Re increases, the evaporation rate gradually decreases. This reduction in evaporation rate is attributed to the increasing liquid film thickness, which raises the thermal resistance of the liquid film and hinders evaporation. However, as Re increases, the flow velocity within the liquid film also increases, leading to a higher falling film heat transfer coefficient. Therefore, in studies on nanofluid enhanced falling film evaporation, it is crucial not only to analyze the falling film heat transfer coefficient but also to examine the evaporation rate from a fundamental perspective.

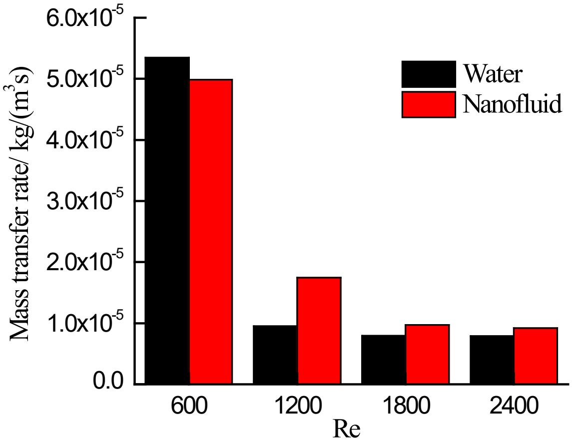

Fig. 5. Mass transfer rate for water and nanofluid

A comparative analysis of the evaporation rates of the nanofluid and water reveals that at Re=600, the evaporation rate of the nanofluid is lower than that of water. However, at Re = 1200, 1800, and 2400, the evaporation rate of the nanofluid exceeds that of water. The influence of the nanofluid on the evaporation rate can be attributed to two main factors: (1) the thermal conductivity of the nanofluid is greater than that of water, which aids in falling film evaporation; (2) the thickness of the nanofluid film is greater than that of the water film, resulting in a significantly higher thermal resistance for the nanofluid, thereby hindering falling film evaporation. At Re = 600, as shown in Figure 3, the significantly thicker nanofluid film leads to a greater thermal resistance, obstructing evaporation more effectively. In contrast, at Re=1200, 1800, and 2400, as depicted in Figure 3, the thickness of the nanofluid film approaches that of the water film, allowing the relative increase in the thermal conductivity of the nanofluid compared to water to gradually enhance falling film evaporation.

4 Conclusion

This study established a two-dimensional mathematical model for falling film evaporation based on the Volume of Fluid (VOF) method and utilized Fluent software to solve the discretized mesh. The analysis focused on the effects of adding 3% aluminum oxide (Al_2O_3) nanoparticles on the liquid film thickness, heat transfer coefficient, and evaporation rate within the Re range of 600 to 2400. The specific conclusions are as follows:

The viscosity of the nanofluid is higher than that of water, which hinders the spread of the liquid film and results in increased film thickness. At Reynolds numbers of 600, 1200, 1800, and 2400, the film thickness of the nanofluid compared to water increased by -27.31% to 36.99%, 1.99% to 14.71%, 3.02% to 9.34%, and 1.98% to 9.73%, respectively.

As the Reynolds number increases, the average temperature of the nanofluid and water outside the horizontal pipe first rises, reaching a peak at Re=1200, and then gradually decreases when Re exceeds 1200.

With the increase in Re, the liquid film thickness gradually increases, and the rise in thermal resistance of the liquid film hinders evaporation. Consequently, the evaporation rate decreases as Re increases. A comparative analysis of the evaporation rates of the nanofluid and water reveals that at Re=600, the evaporation rate of the nanofluid is lower than that of water; however, at Re=1200, 1800, and 2400, the evaporation rate of the nanofluid surpasses that of water.

References

1. S. Sehgal, J. L. Alvarado, I. G. Hassan, et al., "A comprehensive review of recent developments in falling-film, spray, bubble and microchannel absorbers for absorption systems," Renewable and Sustainable Energy Reviews, vol. 142, p. 110807, 2021.
2. A. Nasr, S. A. Bawazeer, "Evaporation of CuO/H2O nanofluid film liquid flow downward in a vertical parallel plate evaporator by mixed convection," Desalination and Water Treatment, vol. 303, pp. 171–180, 2023.
3. A. A. Eidan, A. Alsahlani, M. J. Alshukri, et al., "Experimental investigation of a solar evacuated tube collector embedded with a heat pipe using different nanofluids and controlled mechanical exciting pulsations," International Journal of Thermofluids, vol. 20, p. 100415, 2023.
4. L. Hoffmann, I. Greiter, A. Wagner, et al., "Experimental investigation of heat transfer in a horizontal tube falling film absorber with aqueous solutions of LiBr with and without surfactants," International Journal of Refrigeration, vol. 19, no. 5, pp. 331–341, 1996.
5. H. Qi, "Experimental Study on Mass Transfer Characteristic of Nano Lithium Bromide Solution Added Vapor of Additive," Doctoral Dissertation, Beijing University of Civil Engineering and Architecture, 2015.
6. W. Jiang, S. Li, L. Yang, et al., "Experimental investigation on performance of ammonia absorption refrigeration system with TiO2 nanofluid," International Journal of Refrigeration, vol. 98, pp. 80–88, 2019.
7. Y. Xuan and W. Roetzel, "Conceptions for heat transfer correlation of nanofluids," International Journal of Heat and Mass Transfer, vol. 43, no. 19, pp. 3701–3707, 2000.
8. X. Zhang, "Numerical analysis on microscopic heat transfer behavior of horizontal-tube falling film evaporation based on VOF method," Doctoral Dissertation, Dalian University of Technology, 2015.
9. H. Hou, Q. Bi, H. Ma, et al., "Distribution characteristics of falling film thickness around a horizontal tube," Desalination, vol. 285, pp. 393–398, 2012.